JOURNAL OF MATERIALS SCIENCE **34** (1999) 2843–2849

High temperature fatigue behavior in tensile hold LCF of near-alpha Ti-1100 with lamellar structure

D. H. LEE, S. W. NAM*
Department of Materials Science and Engineering, Korea Advanced Institute of Science and Technology, 373-1 Kusong-dong, Yusong-gu, Taejon 305-701, Korea
E-mail: namsw@cais.kaist.ac.kr

The effect of various tensile hold times on high temperature LCF behavior of Ti-1100 with a lamellar structure was investigated at 600 °C. It was found that fatigue lives for 10 and 30 min hold times were lower than those in continuous cycle fatigue due to additional creep resulting from stress relaxation during the tensile hold. Creep deformation during hold time resulted in a change of dislocation structure from a planar form to an homogeneous distribution within the α lamellae. An apparent activation energy for creep deformation of about 520 kJ/mol was obtained from the stress relaxation curve and was consistent with results of other near-α titanium alloys. In all cases failures were fatigue-dominated, although creep cavity formation was observed in hold time spcimens.

1. Introduction

Ti-1100, near-α titanium alloy, was recently developed for applications in disks and blades in the compressor sections of advanced gas turbine engines for an improvement of about 50 °C in operating temperature over older conventional titanium alloys such as Ti-6242S and IMI829 [1–3]. Compressor parts in gas turbine engines are subjected to simultaneous cyclic and static loading at high temperatures, and may be degraded by this creep-fatigue interaction. In order to get these materials into practical service, the mechanism by which this degradation occurs must be investigated. However, the effects of creep-fatigue interaction on high temperature low cycle fatigue (HTLCF) behavior in this newly developed titanium alloy, and the damage mechanisms under these complicated loading conditions are not yet clearly understood.

Several investigators [2, 3] have studied the effect of microstructure on the mechanical properties of this alloy and proposed an optimum microstructure having high fatigue and creep resistance. A lamellar structure containing the transformed β phase is suggested as the optimum microstructure in the case of Ti-1100. This optimum microstructure has been determined by independently considering some mechanical properties, including creep and fatigue resistance at high temperature, without considering the interaction of them [2, 3].

Some investigators [4–7] have also conducted fatigue tests with only a relatively short hold time to investigate the effect of creep on fatigue crack growth behavior. However, the interaction of creep and fatigue is not clearly understood.

For the sake of safety and better performance, evaluation of the mechanical properties of materials under the real application conditions is very valuable and necessary. In this study the effect of various tensile hold times on HTLCF behavior of Ti-1100 with fine lamellar structure is investigated, and the damage mechanism under these conditions will be also discussed.

2. Experimental

The chemical composition and β-transus temperature of Ti-1100 are shown in Table I. The β-transus temperature was measured by a combination of DTA analysis and optical microscope observation. To make the prior β grain size as small as possible, the as-received alloy was solution-treated at just above the β-transus temperature, 1020 °C, for 30 min, and then air cooled. Aging treatment for 8 hours at 600 °C was conducted, followed by air cooling.

Low cycle fatigue tests were performed at 600 °C, which is near the operating temperature in real applications, on uniform-gauge specimens with a gauge length of 4.2 mm and a diameter of 3.2 mm. Fully reversed axial strain controlled low cycle fatigue tests were carried out in an air atmosphere using an Instron 1380 with a strain rate of 4×10^{-3} s^{-1}.

For high temperature fatigue tests, a dual elliptical radiant heater was used to heat the specimen and the temperature was maintained within the accuracy ±2 K as measured on the top and bottom of the gauge section. The axial strain was measured using an extensometer attached at the specimen holder situated outside the radiant heater, because the gauge section was surrounded

* Jointly appointed at the Center for the Advanced Aerospace Materials.

TABLE I Chemical composition (wt %) and β transus temperature of Ti-1100 alloy

Alloy	Al	Sn	Zr	Mo	Si	Ti	T (°C)
Ti-1100	6.0	2.7	4.0	0.4	0.45	Bal.	1015

by the heating chamber. For the strain calibration at room temperature, two extensometers are used; one is installed at the specimen holder for strain control and the second one is attached within the gauge length to measure the strain. In this calibration the measured strain is found to be similar to the controlled strain. At high temperature, however, because of the furnace the measurement of the strain in the gauge length is not possible. However, it is thought that, since the specimen gauge length is heated to the highest temperature and has the smallest cross-section, the validity of the strain measurement at room temperature is reliable at the test temperature.

Creep-fatigue tests were also conducted with various tensile hold times at the maximum strain of fully reversed strain-controlled fatigue cycles. Hold times given at tensile peak strain were 2, 10 and 30 min. The fatigue life N_f was defined as the number of cycles which produce a 20% drop in the saturated tensile load. In this study, all fatigue test data reported from the Instron 1380 system output signal were automatically stored by a computer program. A transmission electron microscope (Philips CM 20), scanning electron microscope (JEOL JSM 840A) and optical microscopes were used to observe crack paths, fractured surfaces and damage sustained during the creep-fatigue test.

3. Results and discussion

3.1. Microstructure

The microstructure for near-α Ti-1100 alloy is shown in Fig. 1. The microstructure consists of fine lamellae of transformed β, which is a mixture of acicular α type phase, β matrix and grain boundary α. To maximize fatigue and creep resistance in this alloy, solution heat treatment was conducted at 1020 °C, just above the β transus temperature and below the silicide solvus temperature. It is well-known that fatigue properties are positively affected by a decrease in prior β grain size [8]. On the other hand, according to Styczynski *et al.* [9], decreasing the prior β grain size does not diminish the excellent creep properties of fully lamellar structures. The prior β grain size and lamellar spacing of the investigated alloy are about 180 and 0.5 μm, respectively. Tensile properties at 600 °C are also shown in Table II.

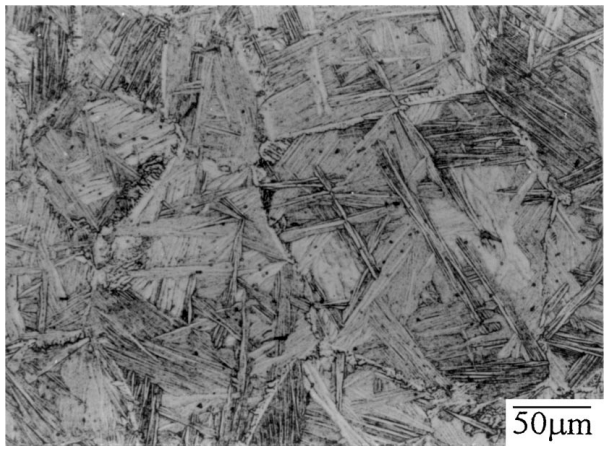

Figure 1 Lamellar microstructure in Ti-1100, solution heat treated for 30 min at 1020 °C.

3.2. Continuous low cycle fatigue behavior

Continuous low cycle fatigue data are plotted in Fig. 2 as a function of total strain range ($\Delta\varepsilon_t$). The results of near-α titanium alloys (Ti-6242, IMI829), superalloy (IN718) and TiAl alloys [10–13], which are competing alloys for high temperature applications, are also shown. Ti-1100 is considered one of the strongest candidate materials for high temperature components of gas turbine engines. From the results in Fig. 2, it can be deduced that fine grained Ti-1100 alloy has a clear advantage in low cycle fatigue life over currently used counterparts at an operating temperature near 600 °C, though the testing temperatures of each alloy were somewhat different.

TABLE II Tensile properties at 600 °C and other physical parameters

YS (MPa)	UTS (MPa)	El. (%)	Prior β grain size (μm)	Lamellar spacing (μm)
535	644	23	180	0.5

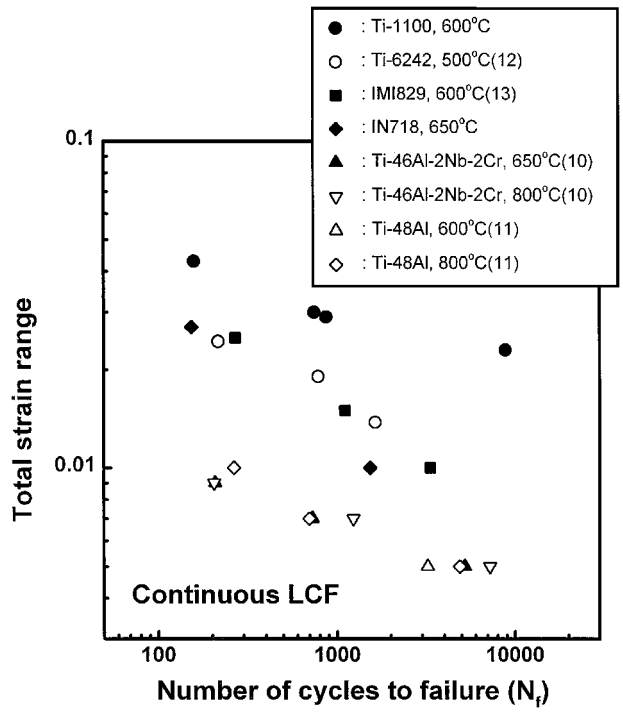

Figure 2 Total strain range plotted against cycles to failure.

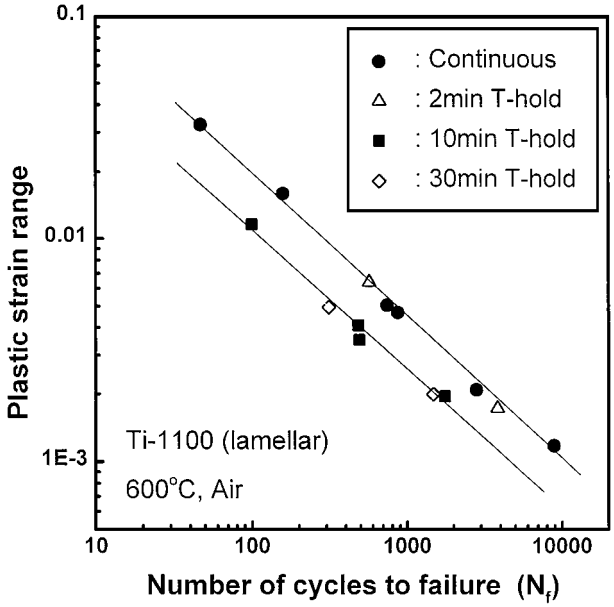

Figure 3 Relationship between plastic strain range and fatigue life, Coffin-Manson plot.

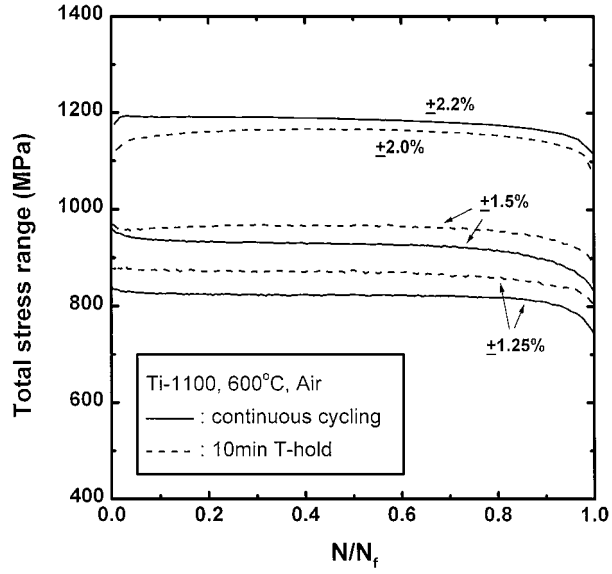

Figure 4 Stress response as a function of strain range and test type.

3.3. Effect of tensile hold time on LCF

The fatigue life data at 600 °C with or without hold time are plotted in Fig. 3 in terms of plastic strain range ($\Delta\varepsilon_p$) against the number of cycles to failure (N_f). The values of plastic strain range for the Coffin-Manson plot were taken from hysteresis loops corresponding to half fatigue life ($N_{f/2}$). In Fig. 3, it can be seen that the Coffin-Manson plots are classified into two groups. One group is for continuous and 2 minute hold time fatigue, and the other group is the test results for 10 and 30 min hold time. It seems likely that in comparison to the longer hold times (10 and 30 min), a tensile hold time of 2 min is too short to cause a genuine effect on creep-fatigue interaction. The data points for 2 min hold time lie on the plot for continuous fatigue. Holding the strain, stress relaxation occurs. In general, the stress relaxes rapidly from σ_{peak} at the early part of hold time and then gradually decreases. Also, it has been noticed that the strain rate associated with the rapid stress relaxation is very fast (about 10^{-5} s^{-1}) during the early part of relaxation and continuously decreases with increasing hold time (about 10^{-7} s^{-1} in a 10 min tensile hold test). So, as the hold time increases, the dominant damage mechanism related with stress relaxation (or strain rate) changes from a time independent process (dislocation glide) to a time dependent process (creep damage). Therefore, σ_{relax} occurring during the first 2 min has little effect on creep damage, and only leads to an increase in the amount of plastic strain mainly by dislocation glide. In other words, it appears that in 2 min hold time fatigue, stress relaxation during hold results in increase of plastic strain which is unrelated with creep damage. Therefore, 2 min hold is not related for the reduction of fatigue life to bring all the datum points on the Coffin-Manson plot of the continuous fatigue.

However, we consider that the reduction in fatigue life from 10 and 30 min hold times is due to additional creep resulting from stress relaxation during the tensile hold. The life reduction factor F_R (= $N_{f,\text{hold time}}/N_{f,\text{continuous}}$), defined as the ratio of fatigue life with hold time to that without hold time, is introduced and it is found that the life reduction factors of Ti-1100 decrease as the hold time increases. For 10 and 30 min tensile hold, the reduction factors of Ti-1100 with lamellar structure at a total strain range of ±1.5% were about 0.6 and 0.4, respectively.

To understand the cyclic response of Ti-1100 alloy, the total stress range is plotted in Fig. 4 against N/N_f, where N represents the cycle number and N_f the cycles to failure. After a slight degree of instability (up to 4%) at the early fatigue life, the overall cyclic stability of Ti-1100 alloy, which differs from other titanium alloys, was generally exhibited during continuous cycling and the hold time tests, as shown in Fig. 4. With this finding, it has been observed that extreme cyclic stability is exhibited in near-α Ti alloys such as IMI829 [14, 15] and IMI834 alloy [16]. Plumbridge and Stanley [14, 15] have reported that cyclic stability of IMI829 alloy appears insensitive to either strain range, test temperature (room temperature and 600 °C), microstructure (basketweave and aligned structure) or hold time. They suggested that it is attributable to the ability of the aligned α colonies to accommodate plasticity. Therefore, it seems that the cyclic stability is characteristic of this kind of near-α Ti alloys.

Depending on the damaging mechanism under creep-fatigue conditions, many high temperature materials have been classified into two different failure modes [17–22]. One such mode is grain boundary cavitation [17–20], and the other is crack-tip deformation which is proposed in terms of concentrated strain within the process zone under creep-fatigue interaction [21]. The former is the group of austenitic stainless steels, while the latter is that of Cr-Mo(-V)-type steels and superalloys. However, there have been no reports on damage mechanisms under creep-fatigue condition in Ti-based alloys. So, attempts have been made to understand the damage mechanism in creep-fatigue interaction of Ti-1100 through TEM examination and the analysis of stress relaxation curves.

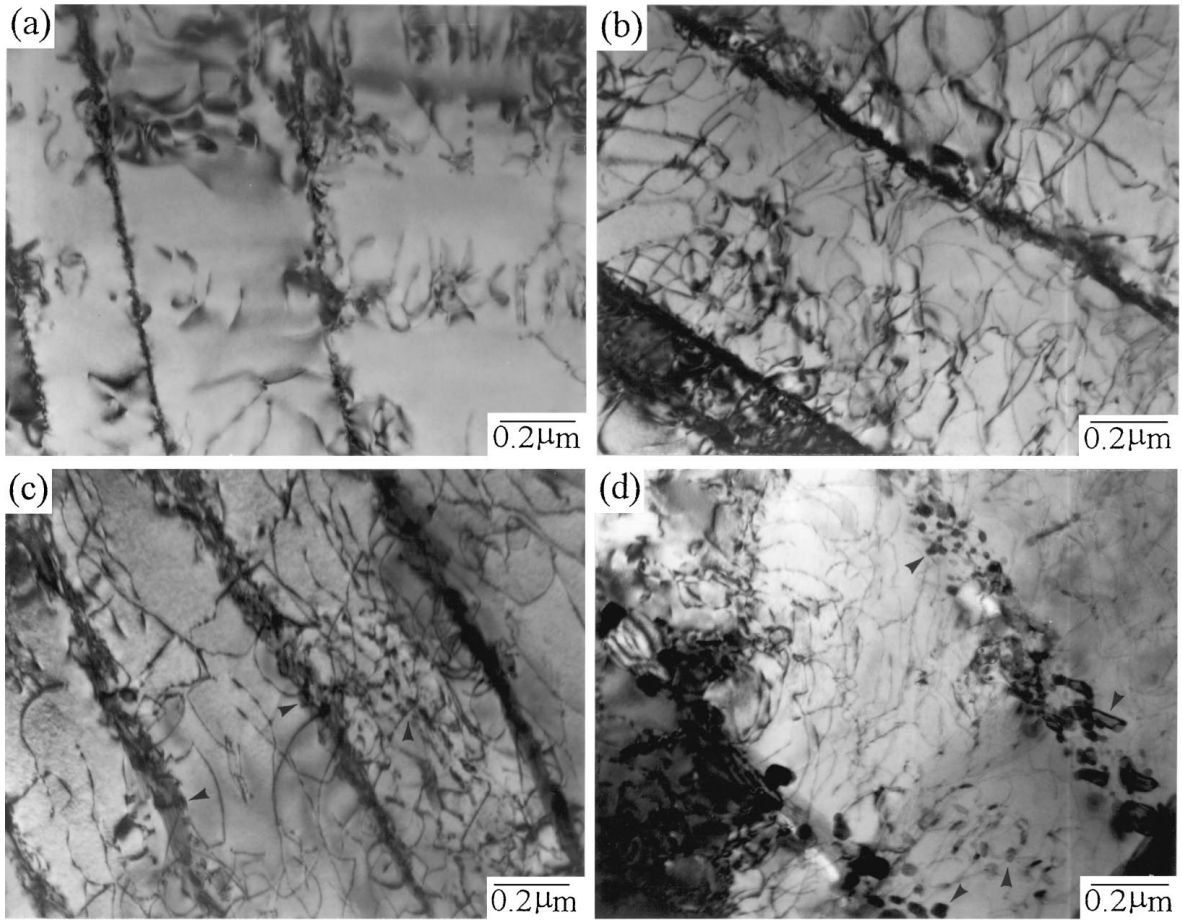

Figure 5 TEM micrographs showing dislocation structure of Ti-1100 alloy with lamellar structure cyclically deformed at $\Delta\varepsilon_t = \pm 1.5\%$: (a) Continuous fatigue, $B = [1\bar{2}1\bar{3}]$; (b) 2 min tensile hold, $B = [1\bar{2}1\bar{3}]$; (c) 10 min tensile hold, $B = [1\bar{2}1\bar{3}]$; (d) 30 min tensile hold, $B = [01\bar{1}1]$. Arrows identify the silicide particles.

In specimens which were cyclically deformed until failure (N_f), the distribution of glide dislocations in the lamellar structure was studied by TEM on thin foils normal to the stress axis (shown in Fig. 5). Inhomogeneous dislocation distribution was dominant in the continuously cyclically deformed specimen. Dislocations were arranged in a planar form across the α/β lamellar interface. Since there was a Burgers orientation relationship ($\{1\,1\,0\}_\beta // (0\,0\,0\,1)_\alpha$, $\langle 1\,1\,1\rangle_\beta // \langle 1\,1\,\bar{2}0\rangle_\alpha$) at the α/β lamellar interface [23], the α/β lamellar interface did not act as an effective barrier to dislocation motion and no dislocation pile-ups were observed at the α/β interface. Analysis of the Burgers vectors, using $\vec{g}\cdot\vec{b}$ criteria, indicates that the dislocation arrays, shown in Fig. 5a, mainly consist of $\vec{a}$ $(1/3\langle 1\,1\,\bar{2}\,0\rangle)$ and $\vec{c}+\vec{a}$ $(1/3\langle 1\,1\,\bar{2}\,3\rangle)$ type dislocations.

Deformation modes of Ti-1100 alloy were also studied for conditions of cyclical deformation with tensile hold time. However, it was found that the deformation structures in these creep-fatigue interaction conditions differed from those observed in only cyclically deformed specimens. That is, no planar slip across the α/β lamellar interface was observed, but dislocations appeared to be homogeneously distributed as shown in Fig. 5b–d. Considering hold time, slip was determined to be random, and occurring within the α lamellae. We consider these phenomena to be responsible for the creep deformation during hold time. According to the previous study [24], continuous cyclic fatigue at room temperature produced long planar slip bands which are extended across several laths and sometimes an entire α colony. But, as the test temperature is increased up to 600 °C, the extended planar slip bands exhibited at room temperature during continuous cycling are changed to an homogeneous dislocation distribution. This finding has been explained to be attributed to the greater ease of cross slip and climb of dislocations arising from the higher temperature. However, in this present study, even at 600 °C, planar slip is observed to be the predominant deformation mode (see Fig. 5a) during continuous cycling.

Also, silicide particles were found to be precipitated along the β phase and on dislocations within the α lamellae in the specimens tested with hold time. It has been reported that the nucleation and growth of these silicide precipitates are accelerated by cyclic straining with hold time. However, in the case of continuous cycling at 600 °C, since the test time was not long enough it was reported to be insufficient for any visible precipitation to occur [24]. This interaction between silicide and dislocations appears to obstruct dislocation movement during the creep deformation related to stress relaxation in this present investigation.

Several researchers [25, 26] have reported that in creep tests, deformation occurs by dislocation movement within α lamellae of the fully lamellar microstructures; this is also observed in the hold time specimens in the present study. It is considered that during the hold

time, creep damage related to stress relaxation occurs through the generation and annihilation of dislocations at the α/β lamellar interface. Therefore, it is thought that this creep damage accelerates crack initiation at the α/β lamellar interface and colony boundary and thus reduces fatigue life.

In order to identify the characteristics of creep deformation during stress relaxation in tensile hold, high temperature low cycle fatigue was conducted at three different temperatures (600, 605 and 610 °C), with 10 min tensile hold. Using the relaxation curve, apparent activation energy for creep deformation was calculated as a function of tensile hold time (shown in Fig. 6). As relaxed stress (or hold time) was increased, the apparent activation energy gradually increased and then saturated at about 520 kJ/mol. This saturated value is consistent with the results of other researchers. Previous studies have reported that activation energies for creep of near-α titanium alloys such as IMI685 and IMI834 are about 250–500 kJ/mol [25, 27, 28], values which are considerably larger than the activation energies for self diffusion (150 kJ/mol) or solute atom diffusion in α titanium (85 to 127 kJ/mol) [28]. This means that creep deformation during hold time in fine lamellar Ti-1100 alloy must be controlled by a mechanism different from that in diffusion-controlled behavior; more detailed investigation related to this finding is necessary.

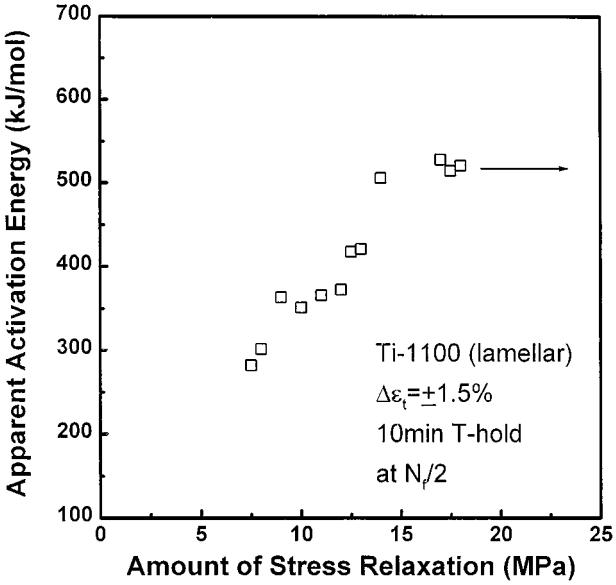

Figure 6 Activation energy for the creep deformation during the hold time, calculated from the stress relaxation curve.

Fig. 7 shows SEM micrographs of fracture surfaces corresponding to different hold times at tensile peak strain. No noticeable difference is found in fracture mode, irrespective of superposition of hold time. Fracture surfaces clearly indicate closely spaced fatigue striations which is a typical ductile fracture mode. It suggests that in all specimens, fatigue cracks initiate at the surface and propagate slowly to considerable depth before final failure occurs.

Optical micrographs in Fig. 8 illustrate the form and overall distribution of damage produced by continuous and hold time fatigue. In both cases, the major fatigue crack path is similarly transgranular. However, as shown in Fig. 8c and d, it was found that internal

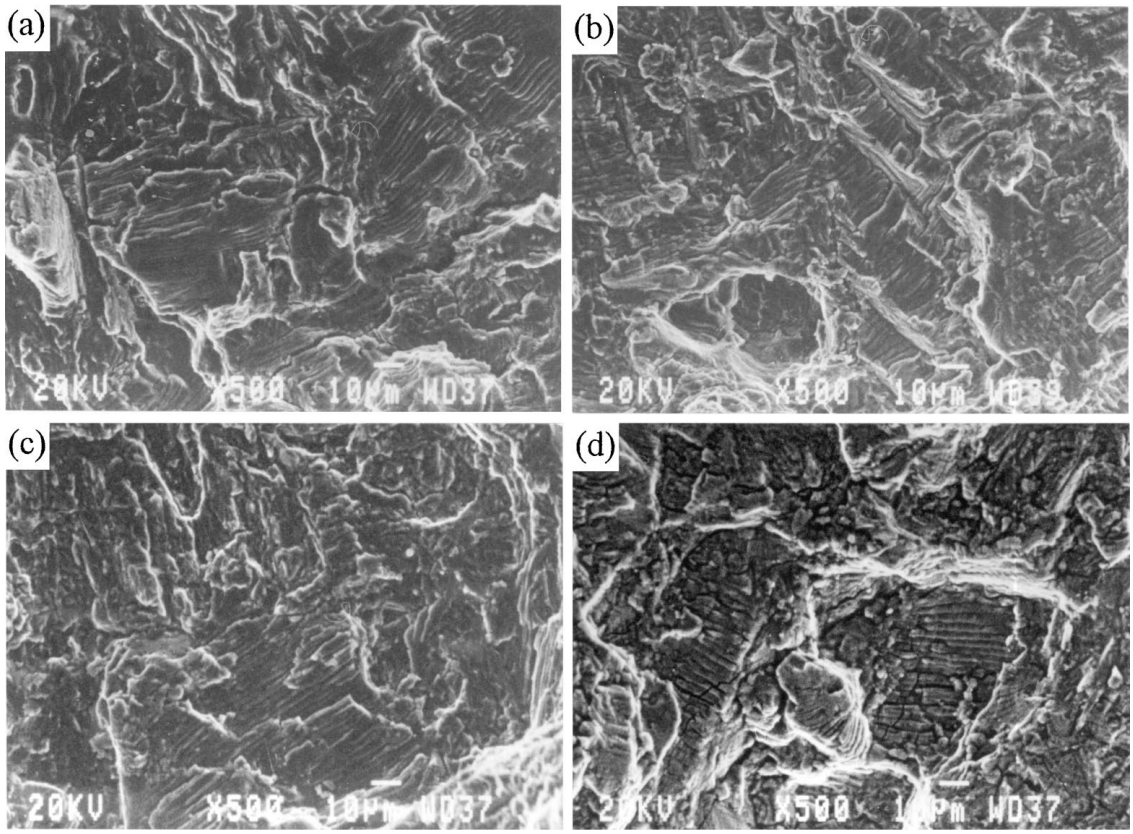

Figure 7 SEM micrographs of the fatigue fractured surface in Ti-1100 alloy with lamellar structure cyclically deformed at $\Delta\varepsilon_t = \pm 1.5\%$: (a) Continuous fatigue; (b) 2 min tensile hold: (c) 10 min tensile hold; (d) 30 min tensile hold.

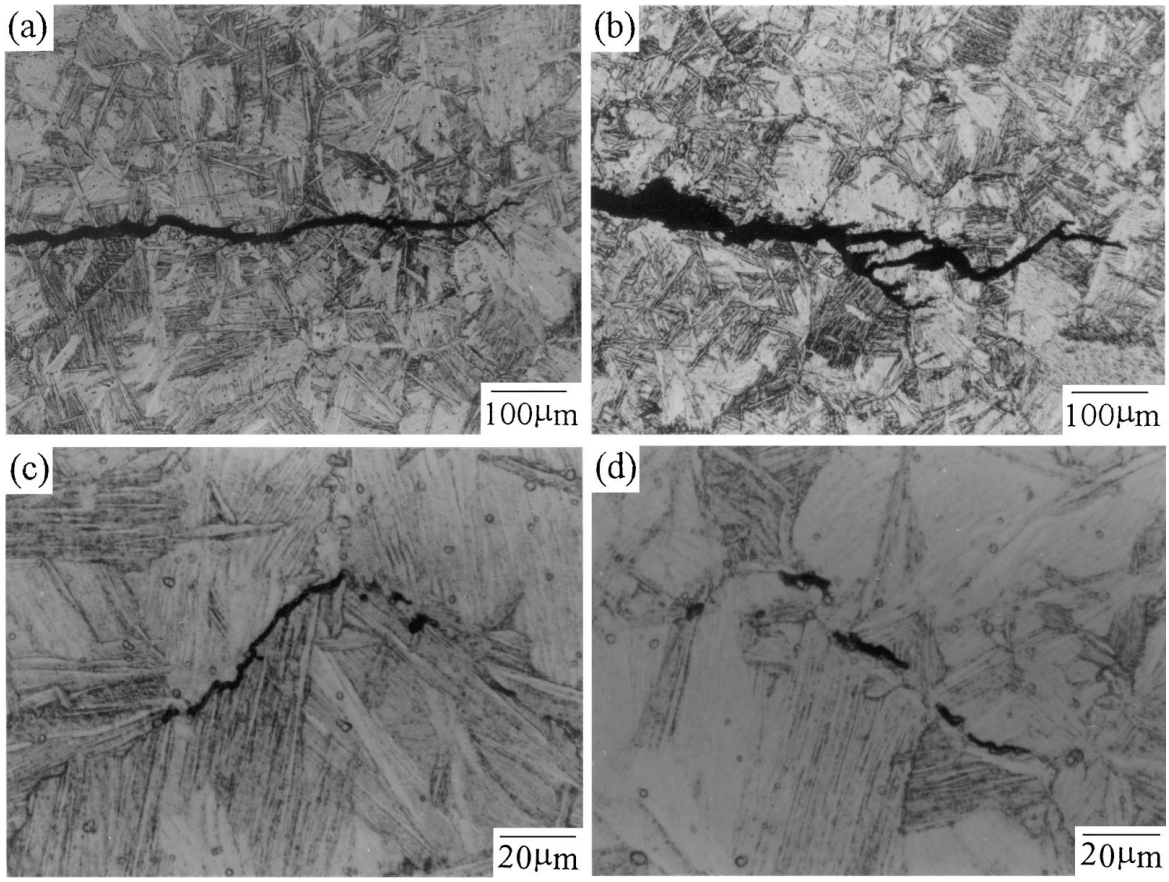

Figure 8 Optical micrographs showing fatigue crack propagation mode of Ti-1100: (a) Continuous fatigue, $\Delta\varepsilon_t = \pm 1.25\%$; (b,c) 10 min tensile hold, $\Delta\varepsilon_t = \pm 1.25\%$; (d) 30 min tensile hold, $\Delta\varepsilon_t = \pm 1.25\%$.

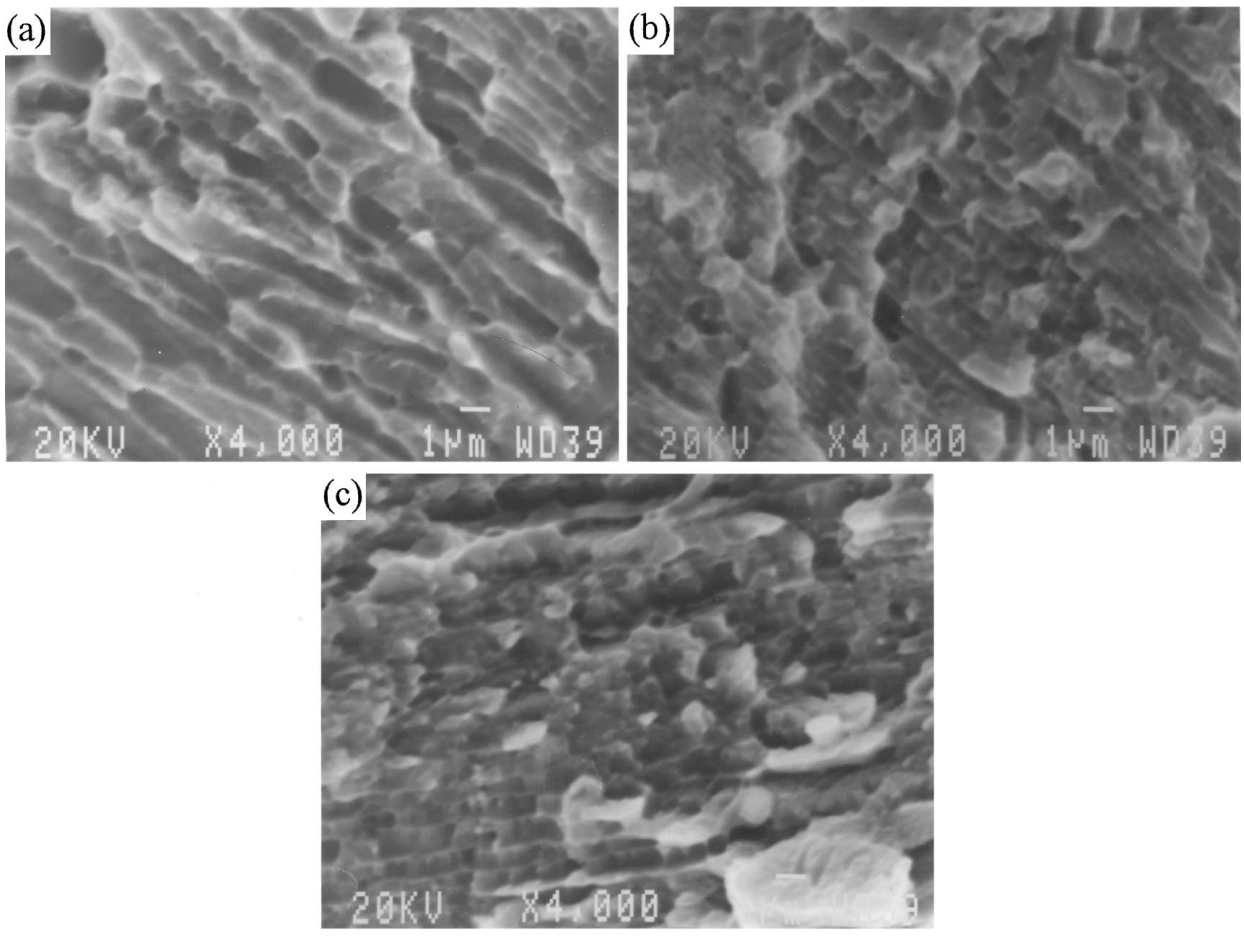

Figure 9 SEM micrographs showing cavities on fracture surface by impact at LNT after creep-fatigue test: (a) Continuous fatigue, $\Delta\varepsilon_t = \pm 1.25\%$; (b) 10 min tensile hold, $\Delta\varepsilon_t = \pm 1.25\%$; (c) 30 min tensile hold, $\Delta\varepsilon_t = \pm 1.25\%$.

cracks regarded as creep damage were produced by cycles containing 10 and 30 min tensile hold. These internal cracks were formed mainly at colony and prior β grain boundaries. In addition to internal cracks in the hold time specimen, the trend of formation of creep cavities is shown in Fig. 9, compared with continuously cycled specimens, which show a fine dimple structure. It seems likely that time-dependent cavity nucleation and growth take place during tensile hold and are closely related to silicide particles (shown in Fig. 5). This creep damage is more pronounced in the longer hold time and lower applied total strain range, because there is more time for creep damage to accumulate. It can be seen that fatigue dominated failures occur at relatively high strain range, while creep failures are predominant at low strain ranges and long hold time. At low strain ranges the surface crack initiation becomes very slow relative to the development of internal creep damage and hence the failure becomes creep dominated. But at very high strain levels, failure becomes fatigue dominated as there is not enough time for the occurrence of creep damage. Therefore, reduction of fatigue life in hold time specimens seems to be to some extent accelerated by creep cavities formed during hold time. However, the significant intergranular failure by grain boundary cavities that has been reported for stainless steels [17–20, 29] was not observed. In the present study, it can be seen that the damage resulting from creep cavities does not play a major role in determining fatigue life during creep-fatigue interaction; all the failures have been fatigue-dominated under the conditions tested. This is in accordance with the findings of Plumbridge and Stanley [13–15], who reported fatigue controlled failure in IMI829 alloy although substantial grain boundary cavitation occurs during tensile only hold time testing. However, if hold time is increased, it is expected that creep damage accumulation would become the dominant failure mode.

4. Conclusions

1. Fatigue lives of near-α Ti-1100 alloy with imposed tensile hold time are smaller than those of high temperature continuous LCF. This can be explained by additive creep deformation during hold time, which leads to a change of dislocation structure from planar form to homogeneous distribution within the α lamellae.

2. The apparent activation energy for creep deformation during tensile hold time obtained from stress relaxation curves, was about 520 kJ/mol, which value was consistent with results of other near-α titanium alloys.

3. It was concluded that the failures were fatigue dominated in the conditions tested. However, in hold time specimens, internal cracks and creep cavities were also observed, and seem to be due to creep deformation resulting from stress relaxation.

Acknowledgements

This work was sponsored by the KOSEF (No: 965-0801-006-2). We are grateful for its financial support. The authors thank Dr. Seung Joo Choe, Department of Materials Engineering at Korea Institute of Machinery and Materials, who donated the alloy.

References

1. P. J. BANIA, *ISIJ International* **31** (1991) 840.
2. M. PETERS, V. BACHMANN, K.-H. TRAUTMANN, H. SCHURMANN, Y. T. LEE and C. H. WARD, Titanium '92 Science and Technology, San Diego, June 1992, edited by F. H. Froes and I. L. Caplan (TMS, Warrendale, 1993) p. 303.
3. P. J. BANIA, Sixth World Conf. on Titanium, Cannes, June 1988, edited by P. Lacombe, R. Tricot and G. Beranger (France, 1989) p. 825.
4. A. H. ROSENBERGER and H. GHONEM, *Fatigue Fract. Eng. Mater. Struct.* **17** (1994) 397.
5. H. GHONEM and R. FOERCH, *Mater. Sci. Eng.* **A138** (1991) 69.
6. B. K. PARIDA and T. NICHOLAS, *Fatigue Fract. Eng. Mater. Struct.* **17** (1994) 551.
7. R. FOERCH, A. MADSEN and H. GHONEM, *Metall. Trans.* **24A** (1993) 1321.
8. A. BERG, J. KIESE and L. WAGNER, Light Weight Alloys for Aerospace Applications III, Las Vegas, February 1995, edited by E. W. Lee, N. J. Kim, K. V. Jata and W. E. Frazier (TMS-AIME, Warrendale, 1995) p. 407.
9. A. STYCZYNSKI *et al.*, Microstructure/Property Relationships of Titanium Alloys, edited by S. Ankem and J. A. Hall (TMS-AIME, Warrendale, 1994) p. 83.
10. G. MALAKONDAIAH and T. NICHOLAS, *Metall. Mater. Trans.* **27A** (1996) 2239.
11. M. TSUTSUMI, R. OHTANI, T. KITAMURA, S. TAKANO and T. OHSHIMA, *J. Soc. Mat. Sci. Japan* **44** (1995) 769.
12. M. HAGIWARA, Y. KAIEDA, Y. KAWABE and S. MIURA, Titanium '92 Science and Technology, San Diego, June 1992, edited by F. H. Froes and I. L. Caplan (TMS, Warrendale, 1993) p. 887.
13. W. J. PLUMBRIDGE, *Fatigue Fract. Eng. Mater. Struct.* **10** (1987) 385.
14. W. J. PLUMBRIDGE and M. STANLEY, *Int. J. Fatigue* **8** (1986) 209.
15. W. J. PLUMBRIDGE and M. STANLEY, Int. Conf. on Fatigue of Engineering Materials and Structures, Sheffield, 1986, p. 377.
16. D. H. LEE and S. W. NAM, Unpublished work.
17. S. W. NAM, Y. C. YOON, B. G. CHOI, J. M. LEE and J. W. HONG, *Metall. Mater. Trans.* **27A** (1996) 1273.
18. J. M. LEE and S. W. NAM, *Int. J. Damage Mechanics* **2** (1993) 4.
19. J. W. HONG, S. W. NAM and K.-T. RIE, *J. Mater. Sci.* **20** (1985) 3763.
20. J. H. HONG, S. W. NAM and S. P. CHOI, *ibid.* **21** (1986) 3966.
21. Y. J. OH and S. W. NAM, *ibid.* **27** (1992) 2019.
22. W. J. OSTERGREN, in Proc. ASME-MPC Symp. on Creep-Fatigue Interaction (ASME, New York, 1976) p. 179.
23. W. G. BURGERS, *Physica* **1** (1934) 36.
24. W. J. PLUMBRIDGE, R. SMITH and G. HUNG DAM, Fatigue 90, edited by H. Kitagawa and T. Tanaka (Material and Component Engineering, 1990) p. 1935.
25. C. ANDRES, A. GYSLER and G. LÜTJERING, *Z. Metallkd.* **88** (1997) 197.
26. W. CHO, J. W. JONES, J. E. ALLISON and W. T. DONLON, Sixth World Conf. on Titanium, Cannes, June 1988, edited by P. Lacombe, R. Tricot and G. Beranger, France, 1989, p. 187.
27. W. J. EVANS and G. F. HARRISON, *J. Mater. Sci.* **18** (1983) 3449.
28. N. E. PATON and M. W. MAHONEY, *Metall. Trans.* **7A** (1976) 1685.
29. P. RODRIGUEZ, K. BHANU SANKARA RAO, *Progress in Materials Science* **37** (1993) 403.

Received 17 June
and accepted 29 December 1998